Purple acid phosphatase *Glyma.12G07500* (*GmPAP14*) mediated internal and external organic phosphorus utilization in soybean

Xia Zhao*, Yihuai Jiang*, Yue Zhou, Wenlong Li, Hui Du, Zhanwu Yang, Xihuan Li, Youbin Kong#, Caiying Zhang#

North China Key Laboratory for Crop Germplasm Resources of Education Ministry, *State Key Laboratory of North China Crop Improvement and Regulation*, *Hebei Key Laboratory of Crop Germplasm Resources*, *Hebei Agricultural University*, *Baoding, 071001*, *China*

Highlights[1]

- *Glyma.12G007500* (*GmPAP14*) was induced in roots and leaves under organic P (Po) condition.
- *GmPAP14* overexpression enhanced secreted and intracellular acid phosphatase activities, leading to higher Pi concentrations in cotyledons, functional leaves and roots under Po condition.
- *GmPAP14* overexpression enhanced internal phosphorus (phosphatidic acid) recycling.

Abstract

Purple acid phosphatases (PAPs) are crucial for plant organic phosphorus (P) utilization. Here, we identified an induced PAP gene, *Glyma.12G007500* (*GmPAP14*), through transcriptional profiling under long-term organic P (Po) condition. *GmPAP14* exhibited significant upregulation across various growth stages in roots and leaves under Po condition. Functional characterization revealed that overexpression of *GmPAP14* enhanced secreted and intracellular acid phosphatase activities, resulting in higher phosphate concentrations in cotyledons, functional leaves and roots under Po condition. Subsequent investigations revealed that the transgenic lines (L1 and L2) with *GmPAP14* overexpression exhibited marked increase in hundred-grain weight and oil content under Po condition. Lipidomic analysis showed that the contents of phosphatidic acid and non-phosphorus galactolipids and sulfolipids were reduced. These metabolic alterations suggested that *GmPAP14* overexpression enhanced internal phosphorus recycling, effectively alleviated phosphorus deficiency symptoms in soybean under Po condition. Overall, these findings demonstrated that *GmPAP14* played a pivotal role in coordinating both internal and external Po utilization, providing a promising target for genetic engineering strategies to improve the phosphorus utilization efficiency in soybean.

Keywords: purple acid phosphatase, organic phosphorus, phosphatidic acid, long-term Po condition, soybean

1. Introduction

Phosphorus (P), one of the three primary macronutrients, plays a pivotal role in plant growth and development. It is a fundamental building block of cellular components, such as nucleic acids, ATP, and other vital compounds. It also participates in photosynthesis, energy transmission and various metabolic pathways (Lambers *et al*. 2015; Zhuang *et al*. 2021). Although there is abundant P in the soil, the majority

#Correspondence Youbin Kong, E-mail: kongyoubin@hebau.edu.cn; Caiying Zhang, E-mail: zhangcaiying@hebau.edu.cn

*These authors contributed equally to the article.

exists as organic phosphorus (Po), such as phytate-P, which accounts for 60–80% of total Po and is unavailable for plant uptake (Wang *et al*. 2021; Wang *et al*. 2024). Therefore, inorganic phosphate (Pi) levels are often inadequate to support optimal crop growth and productivity (Liu 2021; Paz-Ares *et al*. 2022). To achieve high crop yield, excessive phosphate fertilizers are often applied to agricultural fields. However, most applied Pi is not absorbed and utilized by plants. Instead, it becomes immobilized by calcium, iron and aluminum, or is washed away into rivers during rainfall events, leading to soil degradation and aquatic eutrophication (Guan *et al*. 2022; Chen *et al*. 2024). Therefore, enhancing Po acquisition and utilization is crucial for the green and sustainable development of agriculture.

To cope with low-P stress, plants have evolved various adaptive strategies, including alterations in root morphology and architecture, increased acid phosphatase (APase) activity, and the remodeling of membrane lipids (Cong *et al*. 2020; Ding *et al*. 2021; Satheesh *et al*. 2022). The root architectural changes primarily involve reduced primary root growth and significantly increased number and length of lateral roots under low-P conditions. Additionally, plants can enhance P uptake through modifications in root morphology and structure when phosphorus is limited. A recent study has pointed out that overexpression of *GmGDPD2* significantly affects hormone signaling and improves root architecture, phosphate efficiency and yield-related traits (Hu *et al*. 2024). APase, a family of hydrolases ubiquitous in living organisms, hydrolyze organic P to release Pi. Enhanced APase expression and activity represent a key adaptive response in Pi-deprived plants. Through increased APase activity, plants can acquire more P from the soil and remobilize P from senescing tissues (Deng *et al*. 2021; Chai and Schachtman 2022; Lambers 2022).

Purple acid phosphatases (PAPs) are non-specific APases containing a binuclear metal ion center and five conserved motifs (**D**XG/G**D**XX**Y**/G**N**H(D/E)/VXX**H**/G**H**X**H**, bold letters represent invariant residues)(Schenk 1999). To date, several PAP families have been identified in diverse plant species, including 29 PAPs in *Arabidopsis* (Li *et al*. 2002) and 26 PAPs in rice(Zhang *et al*. 2011), 33 PAPs in maize (González-Muñoz *et al*. 2015). Meanwhile, certain genes have been demonstrated to play critical roles in extracellular or intracellular Po utilization. For instance, AtPAP10 (Wang *et al*. 2011; Zhang *et al*. 2014) and AtPAP12 (Robinson *et al*. 2012) contribute to external Po utilization in Arabidopsis under low-P conditions. In rice, OsPAP10a (Tian *et al*. 2012) and OsPAP10c (Lu *et al*. 2016) are essential secreted PAPs in response to low-P stress. Notably, certain PAPs, such as AtPAP26 (Hurley *et al*. 2010) and OsPAP26 (Gao *et al*. 2017) exhibit dual functionality in both external and internal Po utilization. This dual functionality may be vital strategy for improving Po utilization efficiency in plants.

Soybean is a crucial economic crop cultivated worldwide. Due to its nitrogen-fixation property, P deficiency becomes a key limiting factor throughout its growth and development (Zhou *et al*. 2023). To address this challenge, screening P-efficient soybean varieties and identifying key genes have become important strategies. Until now, several PAPs have been identified to play essential roles in enhancing soybean P efficiency. Thirty-five *GmPAPs* were initially identified through the soybean genome database (Li *et al*. 2012). Two genes (*GmPAP7a/7b*) participated in extracellular ATP utilization in soybean (Zhu *et al*. 2020). Overexpression of *GmPAP15a* significantly increased root-associated phytase activity and total P content in hairy roots when phytate-P is supplied as the sole P source (Zhu *et al*. 2023). Metabolomic

analysis found that a group of P-containing metabolites exhibited differential accumulations in mature leaves between wild type (WT) and *GmPAP23* overexpression lines, such as glucose-L-phosphate and trehalose-6-phosphate (Guo *et al*. 2025). Another study demonstrated that GmPAP33 participated in arbuscule degeneration during arbuscular mycorrhizal symbiosis in soybean (Li *et al*. 2019). In our previous work, ectopic expression of *Glyma.12G007500* (*GmPAP14*) enhanced extracellular APase activity and promoted rhizosphere Po acquisition in *Arabidopsis* (Kong *et al*. 2018). However, this gene's functional conservation in soybean--particularly its role in internal Po mobilization—remains uncharacterized. Here, we conducted systematic experiments to elucidate its function in Po utilization in soybean.

2. Materials and methods

2.1. Plant materials and growth conditions

The soybean cultivar zhonghuang 15 (ZH15, P-efficient utilization) was used for gene cloning and expressional analysis. The soybean cultivar Williams 82 was used for transformation to analyze gene and promoter functions. For pot experiments, wild type (WT) and two *GmPAP14* transgenic lines (L1 and L2) were sown in the pots (diameter of 35 cm and height of 40 cm) with low-P soils (total P content 0.5 g kg^{-1}, Pi concentration 7.4 mg kg^{-1}). The Pi and Po treatments in this study were performed using a modified Hoagland solution, supplemented with either 0.137 g L^{-1} KH_2PO_4 (1 mmol L^{-1}, Pi) or 0.11 g L^{-1} phytate-P (1 mmol L^{-1}, Po).

2.2. Expressional analysis of *GmPAP14* in soybean

In this experiment, the tissue-specific expression patterns of *GmPAPs* were analyzed using publicly available transcriptomic data (Libault *et al*. 2010), while their expression profiles under different P conditions were assessed through our RNA-seq data.

For quantitative real-time PCR (qPCR) of *Glyma.12G007500* (*GmPAP14*), the seeds of ZH15 were germinated in a greenhouse under 16 h light (28℃)/8 h dark (24℃) cycles. After 7 days (d) of growth, the seedlings were treated with Pi and Po. Firstly, we collected the first (1-L), second (2-L), third (3-L), and fourth (4-L) trifoliate leaves from the base at 28 d post-treatment to analyze spatial expression of *Glyma.12G007500* (*GmPAP14*). Then, the first leaves from the base were harvested at 7, 14, 21, 28, 35, 42, 49, 56, 63, and 70 d post-treatment to analyze temporal gene expression.

Total RNA was extracted using an Eastep® Super Total RNA Extraction Kit (LS1040) from Promega (USA). Then, the first-strand cDNA was synthesized with a PrimeScript™ Reagent kit and the gDNA Eraser (Takara, Japan). Quantitative RT-PCR (qPCR) was performed with TB Green® Premix DimerEraser™ (RR091A) from Takara Biomedical Technology (Beijing) Co., Ltd. on a CFX96 Real-Time PCR Detection System (Bio-Rad, USA). The primers of *GmPAP14* (5'-TCAAGCAGCCCCTTCATTAG-3' and 5'-AGTTTTCCTT CGGCAATCTTC-3') and *GmActin11* (5'-ATCTTGACTGAGCGTGGTTATTCC-3' and 5'-

GCTGGTCCTGGCTGTCTCC-3') were used in qPCR. Relative expression was calculated using the $2^{-\Delta\Delta Ct}$ method. Three technical replicates were performed for all PCR samples (Livak and Schmittgen 2001).

2.3. Vector construction and plant transformation

In this experiment, total DNA was extracted from the leaves of ZH15 using the cetyltrimethylammonium bromide (CTAB) method. Total RNA was isolated from the roots of ZH15 plants that had been treated under Po condition using Eastep® Super Total RNA Extraction Kit (LS1040) from Promega (USA). Afterward, the promoter and cDNA sequences of *GmPAP14* were cloned.

For gene functional analysis, the cDNA of *GmPAP14* from ZH15 was ligated into pZHAC (containing CaMV 35s promoter, a HA tag and a bar gene) for soybean whole-plant transformation via the *Agrobacterium tumefaciens*-mediated cotyledonary node method (Paz 2004). For the promoter analysis of *GmPAP14*, a 2568-bp *GmPAP14* promoter fragment was inserted into pKGB (containing a bar gene) to construct the *GmPAP14::GUS* vector for soybean transformation using the *Agrobacterium tumefaciens*-mediated cotyledonary node method.

2.4. β-Glucuronidase (GUS) histochemical staining in transgenic soybean

The T_3 transgenic plants with *GmPAP14::GUS* were cultured under Pi and Po conditions. The first (1-L), second (2-L), third (3-L), and fourth (4-L) trifoliate leaves from the base at 28 d post-treatment were harvested for GUS staining. The samples were incubated at 37°C in GUS staining buffer (2 mmol L^{-1} 5-bromo-4-chloro-3-indolylbglucuronic acid in 50 mmol L^{-1} sodium Pi buffer, pH 7.2) containing 0.1% Triton X-100, 2 mmol L^{-1} $K_4Fe(CN)_6$, 2 mmol L^{-1} $K_3Fe(CN)_6$, and 10 mmol L^{-1} EDTA). All the samples were observed and imaged using a SZX7 microscope (Olympus, Japan) and Perfection V800 photo (Epson, Japan).

2.5. Subcellular localization

The cDNA of *GmPAP14* without the stop codon was cloned into pCamE-*GFP* vector to generate *35S-GmPAP14-GFP*. The AtPIP2A-mCherry, as a plasma membrane marker, together with *35S-GmPAP14-GFP* or *35S-GFP* were transformed into 3-week-old tobacco leaves. After incubation for 48 h, the fluorescence was detected using a laser confocal microscope (Zeiss, LSM800 Germany).

2.6. Western blotting

The total proteins of wild-type and transgenic soybeans were extracted by using the Plant Protein Extraction Kit (CW0885M, CWBIO, China). 60-μg protein of each sample was separated by 10% SDS-PAGE gel and transferred to a nitrocellulose filter membrane (10600002, Amersham, USA). The primary antibody (HA Tag monoclonal antibody 1:5000, B1003, Biodragon, China) and the secondary antibody (goat anti-mouse IgG-HRP, 1:5000, BF03001, Biodragon, China) were used for the western blotting. The blotted membrane was detected using an Odyssey FC imaging system (LI-COR, USA).

2.7. Acid phosphatase activity measurement in transgenic soybean

To measure secreted APase activities of roots, 15-day-old seedlings grown under Pi condition were transferred to 150-mL containing 100 mL of a liquid medium supplemented with 1 mmol L ρ-Nitrophenyl Phosphate (ρ-NPP). After being held for 1 day at 24℃, 5 mL of 0.5 mmol L^{-1} NaOH was added to terminate the reaction. Absorbance was measured at 410 nm (Kong *et al*. 2018). APase activity was expressed as ρ-NP released per hour per plant. All experiments were repeated three times, with eight plants per replicate.

To measure APase activities in roots and leaves, the samples were collected for total protein extraction. 20-μL protein of each sample was added to 1-mL ρ-NPP (1 mmol L^{-1}), The reaction was mixed and incubated at 37°C for 1 h. Afterwards, 300-μL solution was mixed with 100-μL Pi reaction buffer (5% ammonium molybdate solution and 10% ascorbic acid; 6:1, v:v). The reaction mixture was incubated at 37°C for 30 min. Pi content was measured at 820 nm with a spectrophotometer. The experiments were repeated three times, with five plants per replicate.

2.8. Pi concentration measurement in transgenic soybean

The transgenic and wild-type (WT) soybean plants were cultured in vermiculite under Pi and Po conditions. The cotyledons, leaves and roots were harvested separately after 30 days under different P treatment. Fresh tissues were then incubated with 100-μL H_2SO_4 (5 mol L^{-1}). Afterwards, 20-μL solution was mixed with 1.48 mL of double distilled water and 500-μL Pi reaction buffer (5% ammonium molybdate solution and 10% ascorbic acid; 6:1, v:v). The reaction mixture was incubated at 37°C for 30 min. P content was measured at 820 nm with a spectrophotometer. The experiments were repeated three times.

2.9. Lipidomics analysis in transgenic soybean

The transgenic line (L2) and wild-type (WT) soybean plants were cultured under Po condition. The first trifoliate leaves from the base at 28 d post-treatment were harvested for lipid extraction. Then, the lipid of each sample was analyzed using UHPLC Nexera LC-30A ultra performance liquid chromatography system (SHIMADZU, Japan) Metabolomic profiling was performed in collaboration with Gene Denovo Biotechnology Co., Ltd. (Guangzhou, China) including mass spectrometry analyses and bioinformatics analysis. The experiments were repeated three biological times.

2.10. Yield-related traits, oil and protein measurements

The wild-type and transgenic lines (L1 and L2) were sown in pot (diameter of 35 cm and height of 40 cm) with low-P soils (total P content 0.5 g kg^{-1}, Pi concentration 7.4 mg kg^{-1}). The seedlings were irrigated with Hoagland solution, supplemented with either KH_2PO_4 (Pi) or phytate-P (Po) once a week until maturity.

Subsequently, yield-related traits were evaluated in compliance with the Guidelines for Regional Trials and Testing of Soybeans in China. The nutritional components of mature seeds, including oil and protein contents, were further quantified using a near-infrared (NIR) spectrometer.

2.11. Data analysis

All data were analyzed using Microsoft Excel 2016 (Microsoft, USA). Student's *t*-test was used to identify differences between the observations. The pictures were drawn in GraphPad Prism 8.0 (GraphPad Software, USA).

3. Results

3.1. *GmPAP14* was significantly upregulated in root and leaf of soybean under Po condition

In this study, we initially analyzed the tissue-specific expression patterns of *GmPAPs* by leveraging publicly available transcriptomic data (Libault *et al*. 2010). The results revealed that six genes, including *Glyma.08G093300*, *Glyma.08G093600*, *Glyma.09G225000*, *Glyma.10G071000*, *Glyma.12G007500*, and *Glyma.18G001300*, exhibited the highest expression levels in root than other members. Within this subset, *Glyma.12G007500* also exhibited higher expression in leaf and pod, while *Glyma.08G093300*, *Glyma.08G093600*, *Glyma.10G071000*, and *Glyma.18G001300* were strongly expressed in nodule (Fig. 1-A). We further examined the expression profiles of these six genes using our own data under Pi and Po conditions. Notably, *Glyma.12G007500* was induced in both root (Fig. 1-B) and leaf (Fig. 1-C) from 28 to 70 days post Po stress (DPP), compared to the other five genes. Subsequently, the sequence of *Glyma.12G007500* was cloned and analyzed, revealing that it was complete identity with our previous *GmPAP14* (Kong *et al*. 2018).

We further quantified *GmPAP14* expression in Zhonghuang15 (ZH15) using quantitative real-time PCR (qPCR). The results showed that *GmPAP14* expression in leaves at different nodal positions was strongly induction under Po condition (Fig. 2-A), with the higher expression observed in the first trifoliate leaves from the base. Additionally, the temporal expression analysis revealed that significant induce of *GmPAP14* in leaves from 21 to 70 DPP, with the peak occurring at 28 DPP (Fig. 2-B), compared with that under Pi condition. Collectively, these results indicate that *Glyma.12G007500* (*GmPAP14*) plays an important role in soybean Po utilization.

3.2. *GmPAP14* promoter was responsive to Po condition

To investigate the regulatory mechanisms of the *GmPAP14* promoter, a 2238-bp promoter fragment was cloned and fused to the β-glucuronidase (*GUS*) reporter gene, generating the *GmPAP14::GUS* construct, which was initially introduced into wild-type soybean plants. Transgenic plants harboring the

GmPAP14::GUS fusion were cultivated under Pi and Po conditions. Subsequently, roots and leaves at different nodal positions were harvested for histochemical GUS staining (Fig. 2-C). The results revealed that GUS staining signals were significantly observed in cotyledons and leaves under Po condition, compared to Pi controls. In addition, more intense GUS staining expanded from vascular bundles to root hairs were observed in roots under Po condition. In contrast, under Pi condition, GUS activity was predominantly localized within the vascular bundles of the roots. These results imply that *GmPAP14* mediates both internal P remobilization and external P acquisition.

3.3. Overexpression of *GmPAP14* significantly enhanced the activities of both internal and external acid phosphatases in soybean plants

To evaluate *GmPAP14*'s role in Po utilization, we generated eight independent T_0 transgenic soybean plants using *Agrobacterium tumefaciens*-mediated cotyledonary node transformation. Two positive transgenic plants were identified by PCR, herbicide resistance screening (Bar test strip), and Western blot validation (Appendix A). Then, they were advanced to the T_3 generation (named L1 and L2) for further functional analysis.

First, we measured the internal and external acid phosphatases (APases) activities of transgenic and wild-type (WT) plants. The results showed that both L1 and L2 had significantly higher internal APase activities in roots (Fig. 3-A) and leaves (Fig. 3-B) than WT. Notably, quantification of secreted APase activity showed that transgenic roots secreted significantly more APase than WT roots (Fig. 3-C), which was consistent with the yellow coloration from ρ-NP staining (Fig. 3-D).

3.4. Overexpression of *GmPAP14* improved the growth of soybean plants under Po condition

To investigate whether the enhanced APase activities in transgenic plants accelerate Po utilization, we conducted further experiments in vermiculite to evaluate plant growth under Pi and Po conditions. Under Po condition, the transgenic lines (L1 and L2) exhibited significantly improved growth compared to WT plants (Fig. 4-A), with plant height increases of 12.2% and 20.6% (Fig. 4-B). Quantitative analysis showed that the two lines had 48.7% and 45.4% increases in fresh weight of shoots (Fig. 4-C), and 11.4% and 11.1% increases in fresh weight of roots (Fig. 4-D), respectively. Furthermore, Pi concentration measurements revealed that overexpression of *GmPAP14* significantly increased Pi levels in cotyledons (Fig. 4-E) and mature leaves of the two lines (Fig. 4-F and G) under Po condition. Meanwhile, the similar results were observed in roots (Fig. 4-H).

3.5. Overexpression of *GmPAP14* enhanced soybean photosynthetic efficiency under Po condition

P deficiency impairs photosynthetic efficiency, which is a major limiting factor for plant productivity. To assess this effect, the WT and transgenic lines (L1 and L2) were planted in pot filled under Pi and Po conditions. The transgenic lines (L1 and L2) showed significant physiological improvements, including higher chlorophyll SPAD values (12.1 and 12.3%, Fig. 5-A) and photosynthetic assimilation rates (16.2 and 18.4%, Fig. 5-B), compared to WT plants under Po condition. Soil P analysis revealed that transgenic lines (L1 and L2) also exhibited significantly enhanced soil P acquisition, with 20.7% (L1) and 13.3% (L2) greater P depletion than WT controls (Fig. 5-C). These results demonstrate that *GmPAP14* overexpression enhances soil Po utilization in soybean.

3.6. Overexpression of *GmPAP14* enhanced soybean agronomic traits under Po condition

At maturity, we measured agronomic traits in both transgenic and WT soybean plants. As shown in Fig. 6-A and F, *GmPAP14* overexpression markedly improved yield-related traits under Po condition. Impressively, the transgenic lines exhibited increased plant height (22.0 and 26.6%), pod number per plant (28.7 and 29.4%), seed number per plant (56.7 and 46.9%), hundred-grain weight (18.8 and 17.9%), and seed weight per plant (87.6 and 77.3%) under Po condition. Meanwhile, we observed increases plant height (33.9 and 37.5%), hundred-grain weight (20.8 and 15.5%), seed weight per plant (30.5 and 34.2%) under Pi condition. Since phosphorus deficiency affects both yield and quality, we analyzed seed composition using near-infrared spectroscopy. Under Po condition, the transgenic lines (L1 and L2) demonstrated increases in oil contents by 1.9 and 1.8%, respectively (Fig. 6-G), while the protein contents in the transgenic lines decreased by 3.5 and 5.0% (Fig. 6-H) compared to WT plants. These comprehensive results demonstrate that overexpression of *GmPAP14* significantly enhances Po utilization in soybean, leading to improved agronomic performance under Po condition.

3.7. The overexpression of *GmPAP14* altered the phospholipid concentrations in soybean leaves under Po condition

Our previous study demonstrated that secreted GmPAP14 enhanced rhizosphere phytic phosphorus utilization (Kong *et al*. 2018). To investigate GmPAP14's role in intracellular P recycling, we performed lipidomic analysis of mature leaves of the WT and transgenic line (L2) under Po condition. Comparative analysis revealed that a total of 32 phospholipid species exhibited differential accumulation between the L2 and WT plants. As illustrated in Fig. 7, L2 displayed a markedly reduced content of phosphatidic acid (PA, 16:0_17:0) under Po condition, compared to WT plants. Conversely, the concentration of triacylglycerol (TAG, 18:1_11:1_11:1 and 45:7e) in L2 was noticeably increased. Furthermore, the amounts of monogalactosyldiacylglycerol (MGDG, 36:8, 38:8, and 36:7), digalactosyldiacylglycerol (DGDG, 28:3e, 30:3e, 46:7, 30:6e, 28:0e, and 25:1), and sulfoquinovosyldiacylglycerol (SQDG, 39:0, 36:6-H, and 36:5-H) in L2 were significantly decreased under Po condition. These lipidomic changes indicate that *GmPAP14*

overexpression promotes phospholipid catabolism while suppressing non-phosphorus galactolipid biosynthesis, thereby optimizing intracellular phosphorus allocation during P deficiency.

4. Discussion

4.1. *Glyma.12G07500* (*GmPAP14*) was induced in both soybean roots and leaves under Po condition

Phosphorus (P) deficiency is a major limiting factor for crop productivity in terrestrial ecosystems, causing an estimated 40% reduction in global agricultural yields (Guo *et al*. 2022). Previous studies have shown that many purple acid phosphatases (PAPs) are induced under Pi-deficient conditions (Li *et al*. 2012; Zhu *et al*. 2020). For instant, *CrPAP1* and *CrPAP5* were induced by the addition of phytate-P in a medium without phosphate salts (Rivera-Solís *et al*. 2013). In this study, an experiment was carried out to investigate the expression profiles of *GmPAPs* in roots and leaves of soybean plants under Pi and Po conditions. The results revealed that *Glyma.12G07500* (*GmPAP14*) was specifically expressed and continuously induced in both tissues under Po condition (Fig. 1), indicating its pivotal role in soybean adaptation to Pi deficiency.

4.2. *GmPAP14* promoter was induced under Po condition

The PHR1 transcription factor is a central regulator of the plant phosphorus (P) deficiency response network(Shi *et al*. 2021). Under Pi deficiency, PHR1 binds to the P1BS cis-element (PHR1-binding site) in downstream gene promoters, activating the expression of P starvation-induced (PSI) genes, including PAPs and phosphate transporters (PTs) (Xue *et al*. 2017). This regulatory mechanism is well-characterized in rice. Bioinformatics analysis revealed that all 26 PAP gene promoters contain P1BS elements, among them, 6 genes were up-regulated after 7 days of low-phosphorus treatment, indicating that they were regulated by OsPHR2 (Zhang *et al*. 2011). In addition, other studies have shown a potential correlation between the number of P1BS elements and induced gene expression levels (Xie and Shang 2018).

In our current study, we analyzed the 1.5-kb promoter regions of *GmPAPs*, and discovered that the majority of *GmPAPs* containing P1BS elements were upregulated under Po condition, which was consist with previous findings. However, we also found that some genes (such as *Glyma.02G117000*, *Glyma.02G192200* and *Glyma.03G262400*) were induced in roots or leaves, despite lacking P1BS motifs, challenging the absolute requirement for P1BS in PHR1-mediated gene activation. Furthermore, we also discovered that during the process of long-term Po condtion, the number of P1BS regulatory elements is not strongly associated with the induced expression levels of genes. For example, *Glyma.12G007500* (*GmPAP14*) maintained near-continuous induction in both roots and leaves with a single P1BS element. In contrast, *Glyma.18G001300* exhibited downregulation or stable expression under identical condition, despite possessing an identical P1BS motif (Appendix B). These results collectively indicate that although PHR1-mediated P1BS recognition serves as the dominant regulatory mechanism for *GmPAPs*, the *GmPAP14*

promoter requires additional cis-regulatory elements for activation under Po condition. This theoretical proposition demands rigorous empirical validation through systematic experimentation in the future.

4.3. GmPAP14 mediated external and internal organic P utilization in soybean

While numerous studies have characterized the roles of intracellular and secreted PAPs play in the utilization of organic phosphorus, only few dual-functional PAPs (AtPAP26 and OsPAP26) reported to mediate both internal and external Po mobilization (Hurley *et al*. 2010; Gao *et al*. 2017). In this study, through extensive tissue analysis and investigation of induced expressions, we discovered that *Glyma.12G007500* (*GmPAP14*) was upregulated in both roots and leaves under Po condition (Fig. 1). Our earlier research has already established that GmPAP14 acts as a secreted purple acid phosphatase (PAP), enhancing the utilization of exogenous phytate in Arabidopsis (Kong *et al*. 2018). In present research, the result of subcellular localization showed that green fluorescence signal of GmPAP14-GFP was mainly enriched in the plasma membrane along with that of AtPIP2A-mCherry (Appendix C). We conducted further experiments specifically in soybean. The enhanced secreted APase activities observed in transgenic soybean plants (Fig. 3-C) and the reduced total phosphorus (P) content in the soil where the transgenic lines grew (Fig. 5-C) further substantiated that overexpression of *GmPAP14* enhanced the Po utilization around the roots of soybean plants. Moreover, prominent GUS staining was detected in the roots and root hairs of transgenic plants carrying the *GmPAP14*::*GUS* construct under Po condition (Fig. 2), offering additional support for this conclusion. Meanwhile, we observed more intense GUS signals in cotyledons and leaves (Fig. 2). Furthermore, our findings revealed that overexpression of *GmPAP14* elevated APase activities in leaves (Fig. 3), resulting in higher inorganic phosphorus (Pi) concentrations in functional leaves (Fig. 4). These findings suggest that GmPAP14 plays a pivotal role in facilitating the utilization of organic phosphorus, both in external and internal environments.

4.4. Phosphatidic acid acted as a GmPAP14 substrate, enabling phosphorus recycling in soybean under Po condition

Purple acid phosphatases (PAPs) exhibit broad substrate specificity, catalyzing the release of inorganic phosphate (Pi) from diverse organic phosphorus (Po) compounds, including nucleotide phosphates (e.g., ADP, ATP) and phytate (Liang *et al*. 2010; Sun *et al*. 2013; Liu *et al*. 2018). Emerging evidence also showed that PAPs involved in phospholipid metabolism (Stigter and Plaxton 2015). For example, GmPAP33 has been biochemically characterized to hydrolyze phosphatidylcholine (PC) and phosphatidic acid (PA) *in vitro* (Li *et al*. 2019). In this study, we demonstrated that GmPAP14 exhibited PA-hydrolyzing capacity in vitro, achieving 97.5% of its ρ-NPP hydrolysis activity (Appendix D). Concurrently, lipidomic analysis revealed a significant reduction in the content of PA (16:0_17:0) in the leaves of the L2 line (Fig. 7). The concentrations of monogalactosyldiacylglycerol (MGDG) and digalactosyldiacylglycerol (DGDG) also exhibited dramatic declines in the leaves of L2, further underscoring that overexpression of *GmPAP14* alleviates Pi deficiency

condition through both external and internal organic phosphorus utilization.

5. Conclusion

Our findings established that *Glyma.12G007500* (*GmPAP14*) was significantly upregulated and actively involved in both external and internal Po utilization. We delineated the functional mode of GmPAP14 in soybean, which included: (i) catalyzing the hydrolysis of phosphatidic acid (PA) in leaves, and (ii) enhancing the utilization of phytate-P derived from the soil (Fig. 8). These insights present GmPAP14 as a potential target for genetic engineering applications aimed at improving soybean phosphorus use efficiency.

Acknowledgements

This research was funded by the S&T Program of Hebei, China (17927670H, 24466301D, and 21326313D).

Declaration of competing interest

The authors declare that they have no conflict of interest.

Declaration of Generative Al and Al-assisted technologies in the writing processs

During the preparation of this manuscript, the authors used Yuanbao (Tencent) to assist in improving the clarity and readability of the language. All content generated was carefully reviewed and revised by the authors as necessary, and the authors take full responsibility for the final content of the article.

References

Chai Y N, Schachtman D P. 2022. Root exudates impact plant performance under abiotic stress. *Trends in Plant Science*, **27**, 80-91.

Chen Q, Zhao Q, Xie B, Lu X, Guo Q, Liu G, Zhou M, Tian J, Lu W, Chen K, Tian J, Liang C. 2024. Soybean (*Glycine max*) rhizosphere organic phosphorus recycling relies on acid phosphatase activity and specific phosphorus-mineralizing-related bacteria in phosphate deficient acidic soils. *Journal of Integrative Agriculture*, **23**, 1685-1702.

Cong W F, Suriyagoda L D B, Lambers H. 2020. Tightening the phosphorus cycle through phosphorus-efficient crop genotypes. *Trends in Plant Science*, **25**, 967-975.

Deng S, Li J, Du Z, Wu Z, Yang J, Cai H, Wu G, Xu F, Huang Y, Wang S, Wang C. 2021. Rice ACID PHOSPHATASE 1 regulates Pi stress adaptation by maintaining intracellular Pi homeostasis. *Plant, Cell & Environment*, **45**, 191-205.

Ding N, Huertas R, Torres J, Ivone, Liu W, Watson B, Scheible W R, Udvardi M. 2021. Transcriptional, metabolic, physiological and developmental responses of switchgrass to phosphorus limitation. *Plant, Cell & Environment*, **44**, 186-202.

Gao W, Lu L, Qiu W, Wang C, Shou H. 2017. *OsPAP26* Encodes a major purple acid phosphatase and regulates phosphate remobilization in rice. *Plant and Cell Physiology*, **58**, 885-892.

González-Muñoz E, Avendaño-Vázquez A O, Montes R A C, De Folter S, Andrés-Hernández L, Abreu-Goodger C, Sawers R J. 2015. The maize (*Zea mays* ssp. *mays* var. B73) genome encodes 33 members of the purple acid phosphatase family. *Frontiers in Plant Science*, **6**, 341.

Guan Z, Zhang Q, Zhang Z, Zuo J, Chen J, Liu R, Savarin J, Broger L, Cheng P, Wang Q, Pei K, Zhang D, Zou T, Yan J, Yin P, Hothorn M, Liu Z. 2022. Mechanistic insights into the regulation of plant phosphate homeostasis by the rice SPX2-PHR2 complex. *Nature Communications*, **13**, 1581.

Guo Q, Zhu S, Lai T, Tian C, Hu M, Lu X, Xue Y, Liang C, Tian J. 2025. A phosphate-starvation enhanced *purple acid phosphatase*, *GmPAP23* mediates intracellular phosphorus recycling and yield in soybean. *Plant, Cell & Environment*, https://doi.org/10.1111/pce.15400.

Guo Z, Cao H, Zhao J, Bai S, Peng W, Li J, Sun L, Chen L, Lin Z, Shi C, Yang Q, Yang Y, Wang X, Tian J, Chen Z, Liao H. 2022. A natural uORF variant confers phosphorus acquisition diversity in soybean. *Nature Communications*, **13**, 3796.

Hu D, Cui R, Wang K, Yang Y, Wang R, Zhu H, He M, Fan Y, Wang L, Wang L, Chu S, Zhang J, Zhang S, Yang Y, Zhai X, Lü H, Zhang D, Wang J, Kong F, Yu D, *et al*. 2024. The Myb73–GDPD2–GA2ox1 transcriptional regulatory module confers phosphate deficiency tolerance in soybean. *The Plant Cell*, **36**, 2176-2200.

Hurley B A, Tran H T, Marty N J, Park J, Snedden W A, Mullen R T, Plaxton W C. 2010. The dual-targeted purple acid phosphatase isozyme AtPAP26 is essential for efficient acclimation of *Arabidopsis* to nutritional phosphate deprivation. *Plant Physiology*, **153**, 1112-1122.

Kong Y, Li X, Wang B, Li W, Du H, Zhang C. 2018. The soybean purple acid phosphatase GmPAP14 predominantly enhances external phytate utilization in plants. *Frontiers in Plant Science*, **9**, 292.

Lambers H, Martinoia E, Renton M. 2015. Plant adaptations to severely phosphorus-impoverished soils. *Current Opinion in Plant Biology*, **25**, 23-31.

Lambers H. 2022. Phosphorus acquisition and utilization in plants. *Annual Review of Plant Biology*, **73**, 17-42.

Li C, Gui S, Yang T, Walk T, Wang X, Liao H. 2012. Identification of soybean purple acid phosphatase genes and their expression responses to phosphorus availability and symbiosis. *Annals of Botany*, **109**, 275-285.

Li C, Zhou J, Wang X, Liao H. 2019. A purple acid phosphatase, *GmPAP33*, participates in arbuscule degeneration during arbuscular mycorrhizal symbiosis in soybean. *Plant, Cell & Environment*, **42**, 2015-2027.

Li D, Zhu H, Liu K, Liu X, Leggewie G, Udvardi M, Wang D. 2002. Purple acid phosphatases of Arabidopsis thaliana: Comparative analysis and differential regulation by phosphate deprivation. *Journal of Biological Chemistry*, **277**, 27772-27781.

Liang C, Tian J, Lam H M, Lim B L, Yan X, Liao H. 2010. Biochemical and molecular characterization of PvPAP3, a novel purple acid phosphatase isolated from common bean enhancing extracellular ATP utilization. *Plant Physiology*, **152**, 854-865.

Libault M, Farmer A, Joshi T, Takahashi K, Langley R J, Franklin L D, He J, Xu D, May G, Stacey G. 2010. An integrated transcriptome atlas of the crop model *Glycine max*, and its use in comparative analyses in plants. *The Plant Journal*, **63**, 86-99.

Liu D. 2021. Root developmental responses to phosphorus nutrition. *Journal of Integrative Plant Biology*, **63**, 1065-1090.

Liu P, Cai Z, Chen Z, Mo X, Ding X, Liang C, Liu G, Tian J. 2018. A root-associated purple acid phosphatase, SgPAP23, mediates extracellular phytate-P utilization in *Stylosanthes guianensis*. *Plant, Cell & Environment*, **41**, 2821-2834.

Livak K J, Schmittgen T D. 2001. Analysis of relative gene expression data using real-time quantitative PCR and the $2^{-\Delta\Delta CT}$ method. *Methods*, **25**, 402-408.

Lu L, Qiu W, Gao W, Tyerman S D, Shou H, Wang C. 2016. *OsPAP10c*, a novel secreted acid phosphatase in rice, plays an important role in the utilization of external organic phosphorus. *Plant, Cell & Environment*, **39**, 2247-2259.

Paz M M, Shou H X, Guo Z B, Zhang Z Y, Banerjee A K, Wang K. 2004. Assessment of conditions affecting *Agrobacterium*-mediated soybean transformation using the cotyledonary node explant. *Euphytica*, **136**, 167–179.

Paz-Ares J, Puga M I, Rojas-Triana M, Martinez-Hevia I, Diaz S, Poza-Carrion C, Minambres M, Leyva A. 2022. Plant adaptation to low phosphorus availability: Core signaling, crosstalks, and applied implications. *Molecular Plant*, **15**, 104-124.

Rivera-Solís R A, Peraza-Echeverria S, Echevarría-Machado I, Herrera-Valencia V A. 2013. *Chlamydomonas reinhardtii* has a small family of purple acid phosphatase homologue genes that are differentially expressed in response to phytate. *Annals of Microbiology*, **64**, 551-559.

Robinson W D, Park J, Tran H T, Del Vecchio H A, Ying S, Zins J L, Patel K, Mcknight T D, Plaxton W C. 2012. The secreted purple acid phosphatase isozymes AtPAP12 and AtPAP26 play a pivotal role in extracellular phosphate-scavenging by *Arabidopsis thaliana*. *Journal of Experimental Botany*, **63**, 6531-6542.

Satheesh V, Tahir A, Li J, Lei M. 2022. Plant phosphate nutrition: Sensing the stress. *Stress Biology*, **2**, 16.

Schenk G, Ge Y, Carrington L E, Wynne C J, Searle I R, Carroll B J, Hamilton S, De Jersey J. 1999. Binuclear metal centers in plant purple acid phosphatases: Fe–Mn in sweet potato and Fe–Zn in soybean. *Archives of Biochemistry and Biophysics*, **370**, 183-189.

Shi J, Zhao B, Zheng S, Zhang X, Wang X, Dong W, Xie Q, Wang G, Xiao Y, Chen F, Yu N, Wang E. 2021. A phosphate starvation response-centered network regulates mycorrhizal symbiosis. *Cell*, **184**, 5527-5540.

Stigter K A, Plaxton W C. 2015. Molecular mechanisms of phosphorus metabolism and transport during leaf senescence. *Plants*, **4**, 773-798.

Sun F, Liang C, Whelan J, Yang J, Zhang P, Lim B L. 2013. Global transcriptome analysis of AtPAP2-

overexpressing *Arabidopsis thaliana* with elevated ATP. *BMC Genomics*, **14**, 752.

Tian J, Wang C, Zhang Q, He X, Whelan J, Shou H. 2012. Overexpression of *OsPAP10a*, a root-associated acid phosphatase, increased extracellular organic phosphorus utilization in rice. *Journal of Integrative Plant Biology*, **54**, 631-639.

Wang L, Li Z, Qian W, Guo W, Gao X, Huang L, Wang H, Zhu H, Wu J W, Wang D, Liu D. 2011. The Arabidopsis purple acid phosphatase AtPAP10 is predominantly associated with the root surface and plays an important role in plant tolerance to phosphate limitation. *Plant Physiology*, **157**, 1283-1299.

Wang Y, Chen Y F, Wu W H. 2021. Potassium and phosphorus transport and signaling in plants. *Journal of Integrative Plant Biology*, **63**, 34-52.

Wang Y, Peng X, Lian X, Yu Q, Zhang L, Li T, Luo H, Yu K, Zhang W, Zhong D. 2024. Natural variation in *ZmGRF10* regulates tolerance to phosphate deficiency in maize by modulating phosphorus remobilization. *The Crop Journal*, **12**, 1414-1425.

Xie L, Shang Q. 2018. Genome-wide analysis of purple acid phosphatase structure and expression in ten vegetable species. *BMC Genomics*, **19**, 646.

Xue Y B, Xiao B X, Zhu S N, Mo X H, Liang C Y, Tian J, Liao H, Miriam G. 2017. *GmPHR25*, a *GmPHR* member up-regulated by phosphate starvation, controls phosphate homeostasis in soybean. *Journal of Experimental Botany*, **68**, 4951-4967.

Zhang Q, Wang C, Tian J, Li K, Shou H. 2011. Identification of rice purple acid phosphatases related to phosphate starvation signalling. *Plant Biology*, **13**, 7-15.

Zhang Y, Wang X, Lu S, Liu D. 2014. A major root-associated acid phosphatase in *Arabidopsis*, AtPAP10, is regulated by both local and systemic signals under phosphate starvation. *Journal of Experimental Botany*, **65**, 6577-6588.

Zhou M, Li Y, Lu X, He P, Liang C, Tian J. 2023. Diverse functions of GmNLA1 members in controlling phosphorus homeostasis highlight coordinate response of soybean to nitrogen and phosphorus availability. *The Crop Journal*, **11**, 1251-1260.

Zhu S, Chen M, Liang C, Xue Y, Lin S, Tian J. 2020. Characterization of purple acid phosphatase family and functional analysis of *GmPAP7a/7b* Involved in extracellular ATP utilization in soybean. *Frontiers in Plant Science*, **11**, 661.

Zhu S, Guo Q, Xue Y, Lu X, Lai T, Liang C, Tian J. 2023. Impaired glycosylation of GmPAP15a, a root-associated purple acid phosphatase, inhibits extracellular phytate-P utilization in soybean. *Plant, Cell & Environment*, **4**, 272-279.

Zhuang Q, Xue Y, Yao Z, Zhu S, Liang C, Liao H, Tian J. 2021. Phosphate starvation responsive GmSPX5 mediates nodule growth through interaction with GmNF‐YC4 in soybean (*Glycine max*). *The Plant Journal*, **108**, 1422-1438.

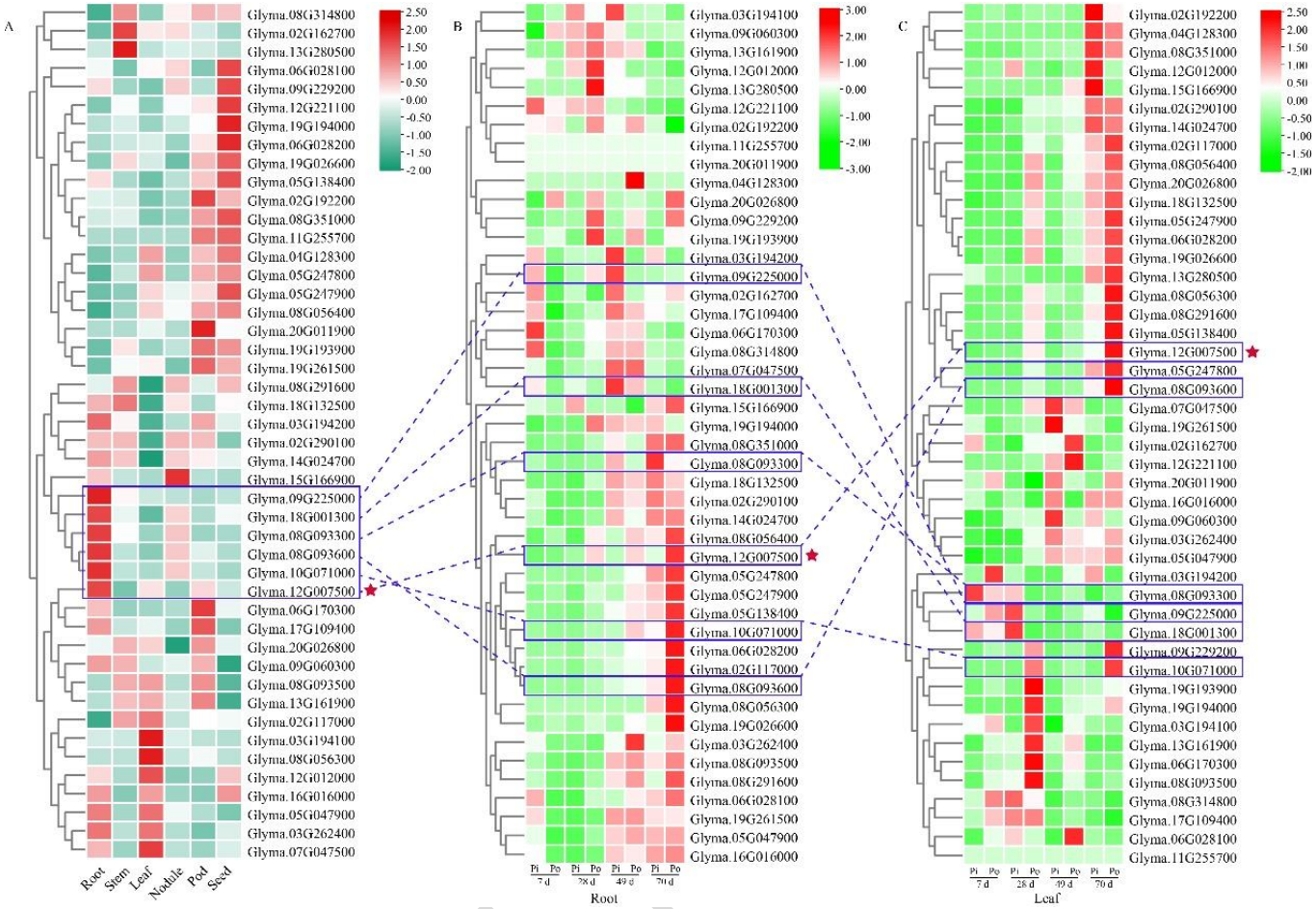

Fig. 1 Expression analysis of *GmPAPs* in soybean under Pi and Po conditions. A, expression of *GmPAPs* in different tissues. RNA-seq data (Libault *et al*. 2010) were shown as a heat map. The color scheme used to represent the expression level were red and blue: red indicated a high variation in expression and blue indicated a low variation in expression. B, expression of *GmPAPs* in roots under Pi and Po conditions RNA-seq data from ZH15 roots treated with KH_2PO_4 (Pi) and Phytate-P (Po) are shown as a heat map. The color scheme used to represent the expression level were red and green: red indicated a high variation in expression and green indicated a low variation in expression. C, expression of *GmPAPs* in leaves under Pi and Po conditions. RNA-seq data from ZH15 leaves treated with KH_2PO_4 (Pi) and Phytate-P (Po) are shown as a heat map. The color scheme used to represent the expression level were red and green: red indicated a high variation in expression and green indicated a low variation in expression. blue box indicated higher expression genes in root (*Glyma.08G093300*, *Glyma.08G093600*, *Glyma.09G225000*, *Glyma.10G071000*, *Glyma.12G007500*, and *Glyma.18G001300*). Red star indicated *Glyma.12G007500* (*GmPAP14*).

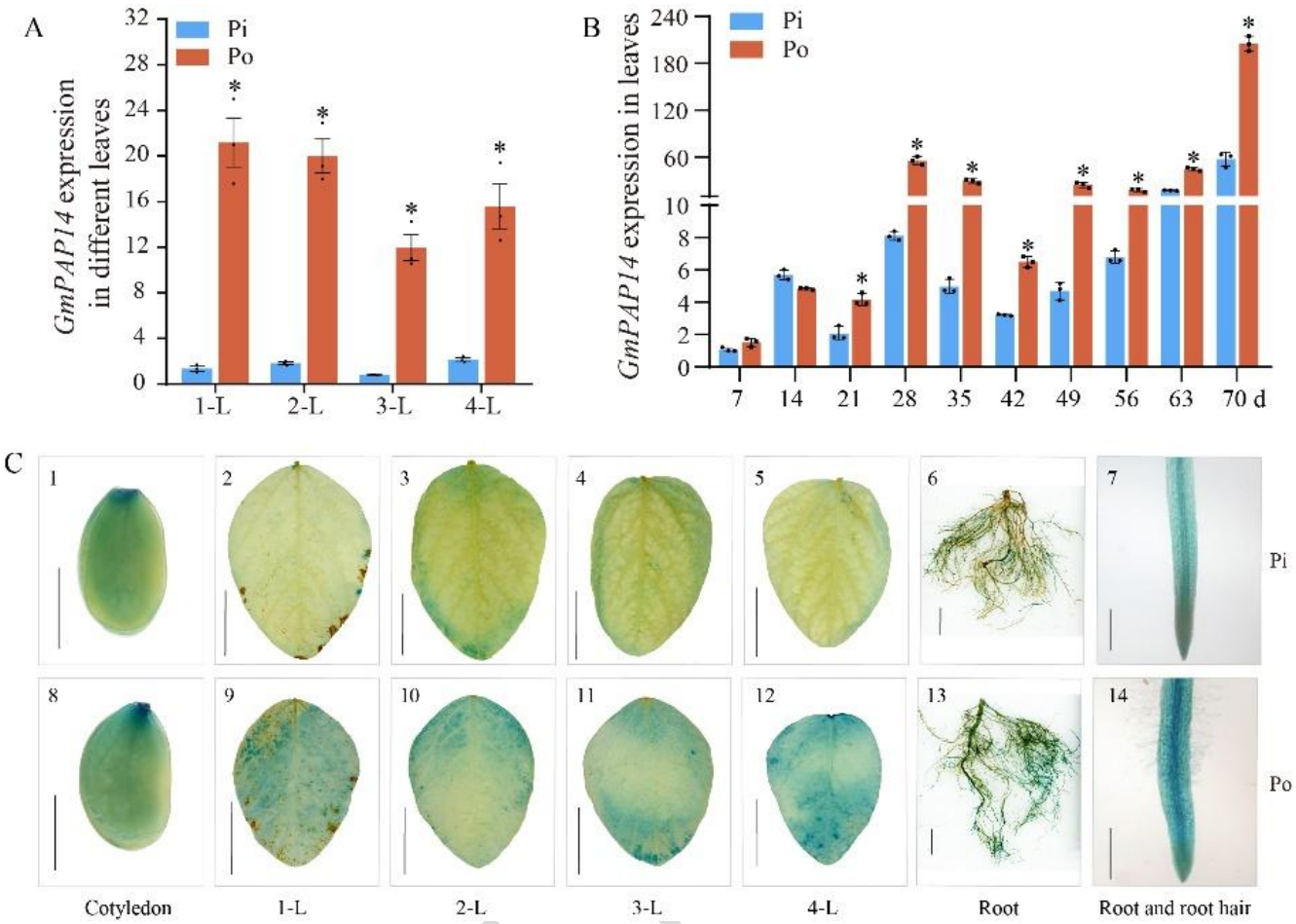

Fig. 2 Analysis of *GmPAP14* and its promoter activity in soybean under Pi and Po conditions. A, analysis of *GmPAP14* expression in leaves at different nodes under Pi and Po conditions. B, analysis of *GmPAP14* expression in leaves under Pi and Po conditions. The plants were sowed in vermiculite and treated with KH_2PO_4 (Pi) and Phytate-P (Po). After 7 d, 14 d, 21 d, 28 d, 35 d, 42 d, 49 d, 56 d, 63 d, 70 d, the samples were harvested for temporal expression in root and leaves using qPCR. The leaves at different nodes were harvested for spatial expression at 28 d post-treatment (1-L, the first trifoliate leaves from the base; 2-L, the second trifoliate leaves from the base; 3-L, the third trifoliate leaves from the base; 4-L, the fourth trifoliate leaves from the base trifoliate leaves). The significant differences of *GmPAP14* expression at the same growth period under Pi and Po conditions (* indicates $P<0.05$, *t*-test). The relative expression value was calculated by the ratio of the expression value of *GmPAP14* to that of soybean housekeeping gene *GmActin11* using the $2^{-\Delta\Delta Ct}$ method. Each bar is the mean of three replicates with the standard error. C, analysis of *GmPAP14* promoter under Pi and Po conditions. Cotyledons, leaves at different nodes and roots were harvested for GUS staining. 1-L, leaves at the first node; 2-L, leaves at the second node; 3-L, leaves at the third node; 4-L, leaves at the fourth node. 1-6, 8-13, the scale bar=1 cm. 7 and 14, the scale bar=500 μm.

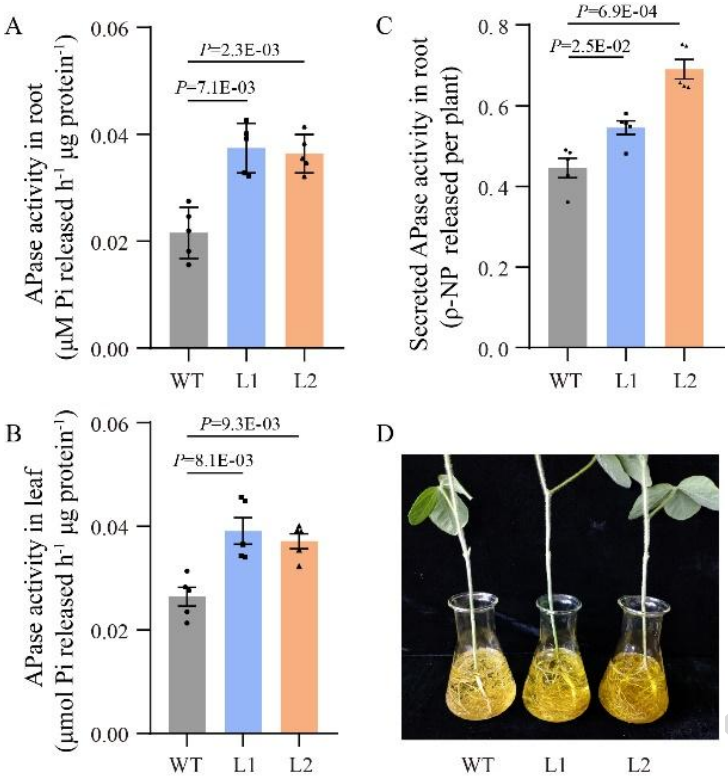

Fig. 3 Measurements of internal and secreted enzyme activities. A and B, internal APase activities in roots and leaves of transgenic (L1 and L2) and wild-type (WT) soybean plants. The protein was extracted from 15-day-old seedling under Pi condition. The reaction was mixed with 1-mL ρ-NPP (1 mmol L^{-1}), and incubated at 37°C for 1 h. The reaction was incubated with a Pi reaction buffer and measured at 820 nm with a spectrophotometer. Data represent the mean±SE (n=5). C, secreted enzyme activities of transgenic (L1 and L2) and wild-type (WT) soybean plants. 15-day-old seedlings under Pi condition were transferred to 150-mL Eppendorf tubes containing 100 mL of a liquid medium supplemented with 1 mmol/L ρ-NPP. After being held for 1 d at 24°C. APase activities were measured at 410 nm. APase activity was expressed as ρ-NP released per hour per plant. Data represent the mean±SE (n=8). Error bars represented SE for all samples tested. Student's t-test was used to identify differences between the data.

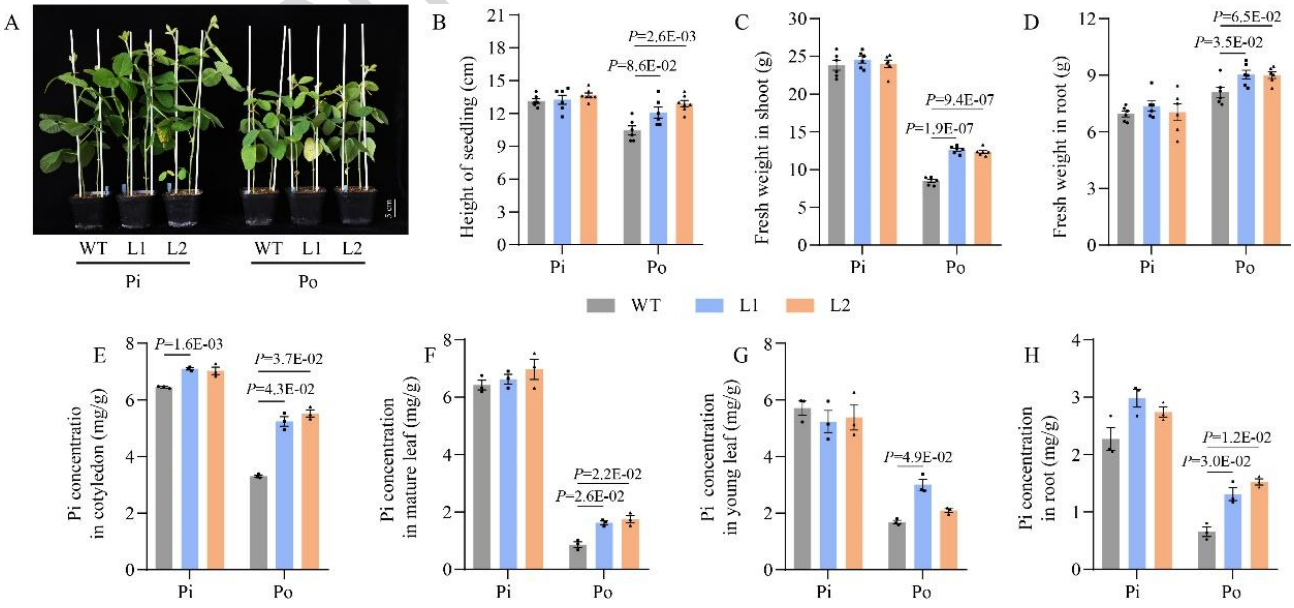

Fig. 4 Phenotypic and Pi concentration analysis of transgenic plants under Pi and Po conditions. A, appearance of

30-day-old seedlings after treatment with KH_2PO_4 (Pi) and Phytate-P (Po). (B) Height of seedling analysis. C and D, fresh weights of shoot and root analysis. Data represent the mean±SE (n=6). E, Pi concentration in cotyledon analysis. F, Pi concentration in mature leaf. G, Pi concentration in young leaf. H, Pi concentration in root. L1 and L2, transgenic plants. WT, the wild-type plants. Data represent the mean±SE (n=3). Error bars represented SE for all samples tested. Student's t-test was used to identify differences between the data.

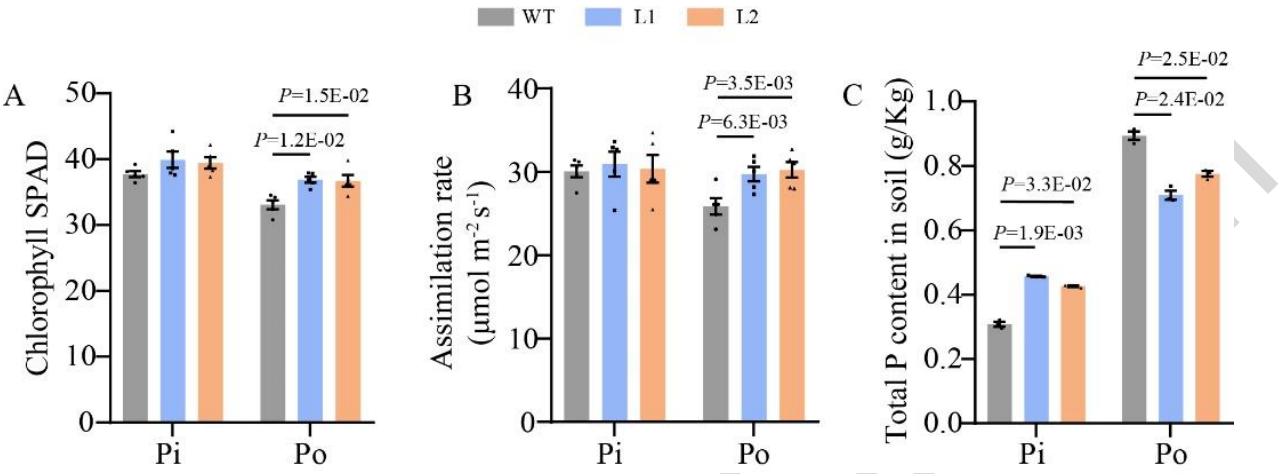

Fig. 5 Measurements of photosynthetic efficiency in transgenic plants under Pi and Po conditions. A, chlorophyll SPAD measurements of transgenic (L1 and L2) and wild-type (WT) soybean plants. B, assimilation rates of transgenic (L1 and L2) and wild-type (WT) soybean plants. C, analysis of the total P contents in soil. Transgenic and WT plants were sown on soil in pot under Pi and Po conditions. After grown 60 d, chlorophyll was measured using SPAD-502 PLUS, and assimilation rate were measured using CIRAS-3. Data represent the mean±SE (n=5 for a and b, n=3 for c). Error bars represented SE for all samples tested. Student's t-test was used to identify differences between the data.

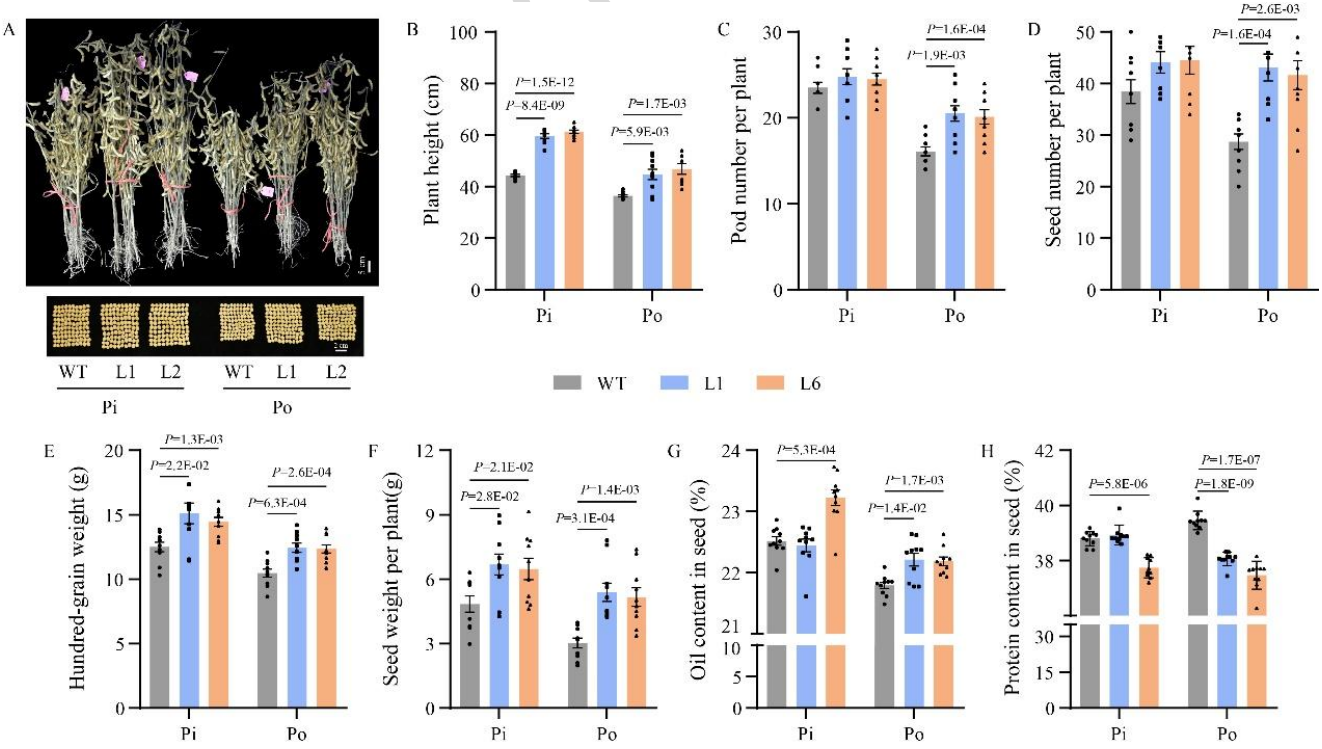

Fig. 6 Agronomic traits analysis of transgenic and wild-type plants under Pi and Po conditions. A, the performance of mature plants under Pi and Po conditions. B, measurement of plant height. C, measurement of pod

number per plant. D, Measurement of seed number per plant. E, Measurement of hundred-grain weight. F, Measurement of seed weight per plant. G, measurement of oil content in seed. H, measurement of protein content in seed. The transgenic (L1 and L2) and wild-type (WT) plans were planted in pot with low-P soil (total P content 0.5 g kg^{-1}, Pi concentration 7.4 mg kg^{-1} in soil). After matured, the measurements of agronomic traits were carried out with reference to the Chinese soybean regional test seed guide. The oil and protein contents in seed were detected using near-infrared spectroscopy instrument. Data represent the mean±SE (n=10). Error bars represented SE for all samples tested. Student's t-test was used to identify differences between the data.

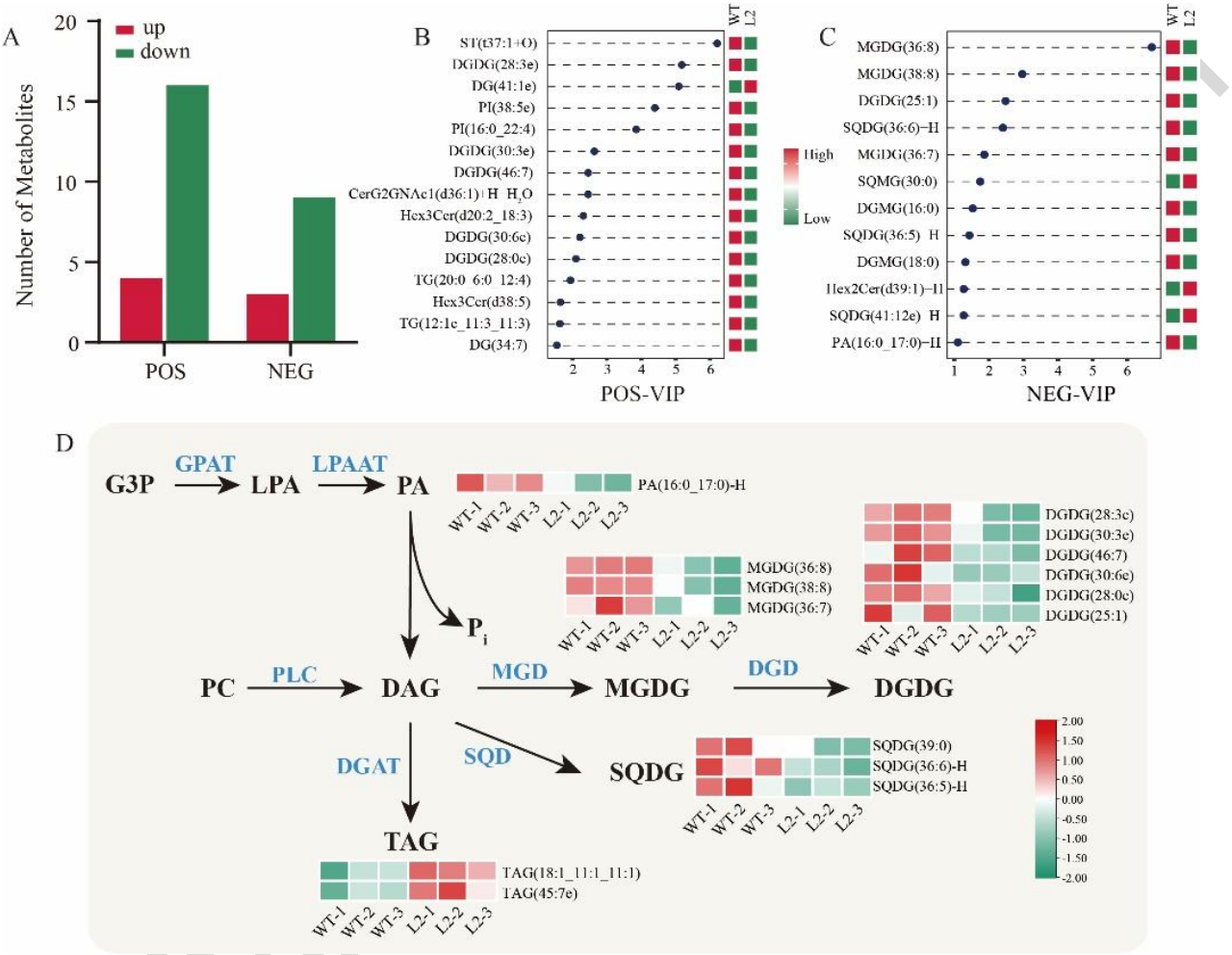

Fig. 7 Analysis of phospholipid metabolism in transgenic and wild-type plants under Po condition. A, number of differential metabolites. B, the content of metabolites in positive ion mode (POS). C, the content of metabolites in negative ion mode (NEG). D, Analysis of the contents of major metabolites in the phospholipid metabolic pathway. The transgenic line (L2) and wild-type (WT) soybean plants were cultured under Po condition. After 30 days, the bottom leaves of the plants were harvested for lipidomics absolute-quantitative analysis. The experiments were repeated three biological times. WT-1/WT-2/WT-3 and L2-1/L2-2/L2-3 represent three biological sample, respectively. The results were shown as a heat map. The color scheme used to represent the expression level were red and blue: red indicated a high content and blue indicated a low content. G3P, glycerol-3-phosphate; GPAT, G3P acyltransferase; LPA, lysophosphatidic acid; LPAAT, lysophosphatidicacidacyltransferase; PA, phosphatidic acid; DAG, diacylglycerol; PC, phosphatidylcholine; PLC, phospholipase C; DAG, diglyceride; MGD, MGDG synthase; DGD, DGDG synthase; MGDG, monogalactosyldiacylglycerol; DGDG, Digalactosyldiacylglycerol; SQDG, Sulfoquinovosyldiacylglycerol;

TAG, triacylglycerol; SQD, SQDG synthase. The abundance of differential lipid in the same group was normalized by z-score. And then, the variable importance in projection (VIP) score of orthogonal projection to latent structures-discriminant analysis (OPLS-DA) was used to draw the graph. The top lipid are shown in the variable importance in projection (VIP) score plot in descending order.

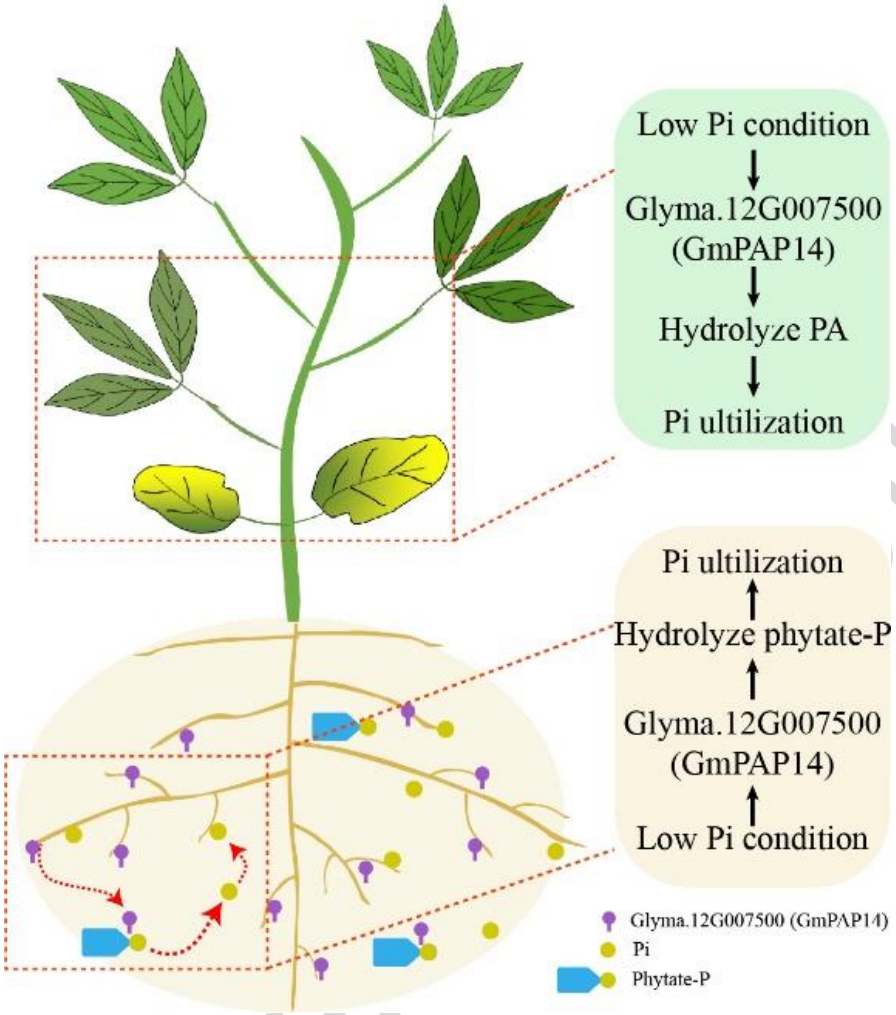

Fig. 8 Schematic representation of Po utilization via GmPAP14-mediated under phosphate (Pi) starvation condition in soybean. Under Pi starvation condition, (i) GmPAP14 was secreted into the rhizosphere soil, where it hydrolyzes phytate-P to release Pi, enhancing Po availability; (ii) it catalyzed the hydrolysis of PA to Pi, contributing to PA metabolism in in the leaves. Through these two mechanisms, GmPAP14 significantly promoted Po utilization efficiency in soybean.